# Synthetic Gene Network for Entraining and Amplifying Cellular Oscillations

Jeff Hasty,[1] Milos Dolnik,[2] Vivi Rottschäfer,[3] and James J. Collins[1]

[1]*Center for BioDynamics and Department of Biomedical Engineering, Boston University, 44 Cummington Street, Boston, Massachusetts 02215*

[2]*Department of Chemistry and Center for Complex Systems, Brandeis University, Waltham, Massachusetts 01655*

[3]*Mathematical Institute, Leiden University, P.O. Box 9512, 2300 RA Leiden, The Netherlands*

(Received 19 April 2001; published 22 March 2002)

We present a model for a synthetic gene oscillator and consider the coupling of the oscillator to a periodic process that is intrinsic to the cell. We investigate the synchronization properties of the coupled system, and show how the oscillator can be constructed to yield a significant amplification of cellular oscillations. We reduce the driven oscillator equations to a normal form, and analytically determine the amplification as a function of the strength of the cellular oscillations. The ability to couple naturally occurring genetic oscillations to a synthetically designed network could lead to possible strategies for entraining and/or amplifying oscillations in cellular protein levels.

DOI: 10.1103/PhysRevLett.88.148101 PACS numbers: 87.17.–d

The flurry of genomic research has led to detailed lists of the genes that are at the heart of cellular function. These genes and their protein products form a complex web of interactions, wherein the proteins serve to activate or repress the transcription of the genes. The dissection and analysis of the complex dynamical interactions involved in gene regulation is thus a natural next step in genomic research, and tools from nonlinear dynamics and statistical physics will no doubt play an important role.

Although a theoretical framework for analyzing gene networks has origins that date back nearly 30 years [1,2], it is relatively recent that experimental progress has made genetic networks amenable to quantitative analysis [3,4]. This progress has rendered feasible the notion of an engineering-based approach to the study of gene networks [5,6], whereby dynamical modeling tools are used in the design of novel networks that can, in turn, be constructed and studied in the laboratory. Recent examples of this approach [7–9] have yielded observed network behavior which is consistent with predictions that arise from continuum dynamical modeling. Such an inherently reductionist decoupling of a simple network from its native and often complex biological setting can lead to valuable information regarding evolutionary design principles [10], and set the stage for a modular description of the regulatory processes underlying basic cellular function [11,12]. Additionally, this approach could have a significant impact on postgenomic biotechnology. From the construction of simple switches or oscillators, one can envision the design of integrated biological circuits capable of performing increasingly elaborate functions [13].

In this Letter, we describe a model for a synthetic gene oscillator designed from common gene regulatory components. We emphasize how the model equations can be used to develop design criteria for robust oscillations, and couple the synthetic oscillator to an oscillating cellular process. The synthetic oscillator design (Fig. 1) consists of two plasmids, both containing the same promoter (denoted $P^*_{RM}$). On plasmid 1, the promoter controls the *cI* gene and thus regulates the expression of the CI protein. On plasmid 2, the promoter controls the *lac* gene, and thus regulates the production of the Lac protein. Interesting dynamics in the numbers of CI and Lac proteins arises due to the influence of two of the binding configurations on the transcriptional rate: (i) when a CI dimer is bound to OR2 and when $OR3^*$ is vacant (Fig. 1), the promoter is turned "on," that is, its gene is transcribed at an amplified rate, and (ii) when a Lac tetramer is bound to $OR3^*$, the promoter is turned "off," i.e., its gene is not transcribed.

Utilizing the reactions given in Table I and defining concentrations as our dynamical variables, the following rate equations describe the evolution of the concentrations of CI ($X$) and Lac ($Y$) monomers:

$$\begin{aligned}\frac{dX}{d\tau} &= -2k_1X^2 + 2k_{-1}X_2 \\ &\quad + k_t(D^1 + D^1X_2 + \alpha D^1X_2X_2) - k_xX\,, \\ \frac{dY}{d\tau} &= -2k_2Y^2 + 2k_{-2}Y_2 \\ &\quad + k_t(D^2 + D^2X_2 + \alpha D^2X_2X_2) - k_yY\,,\end{aligned} \tag{1}$$

where $X_2$ ($Y_2$) is the concentration of CI (Lac) dimers and the bracketed transcription terms are the concentrations of the DNA and DNA-protein complexes for plasmids 1 (superscript 1) and 2 (superscript 2); see also Table I.

The protein multimers and the complexes can be eliminated by utilizing the inherent separation of time scales; the multimerization processes are known to be governed by rate constants that are extremely fast with respect to cellular growth and transcription (Table I). This allows for algebraic substitution [14] and leads to the following set of equations:

  

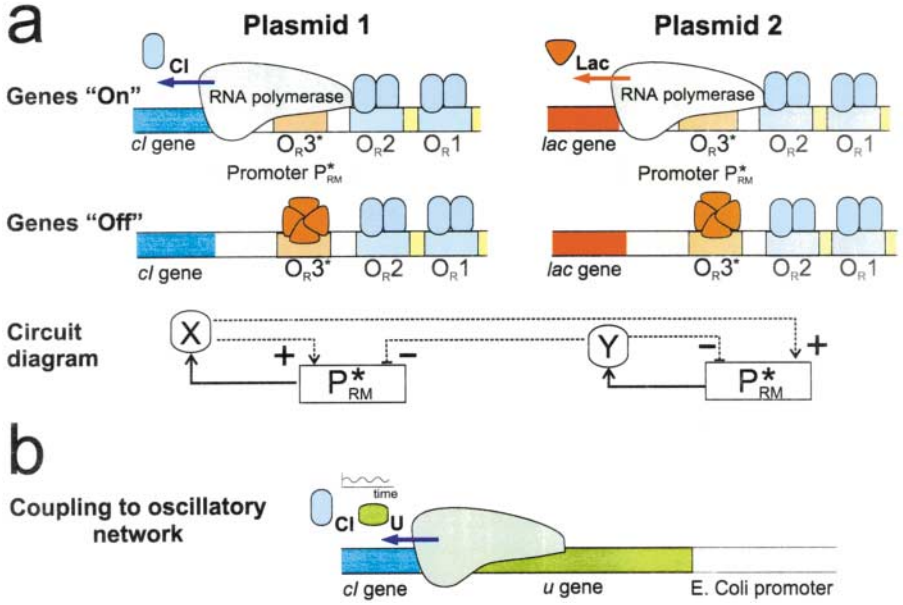


FIG. 1 (color). (a) Schematic for the synthetic gene oscillator. The $P^*_{RM}$ promoter is a mutant of the $P_{RM}$ promoter that naturally exists in the virus $\lambda$ phage [16]. In its natural state, the state of the virus is regulated by CI dimers which bind to the three operator sites OR1, OR2, and OR3; in our design, the OR3 operator is replaced with an operator region OR3* which has an affinity only for Lac tetramers. The depicted position of the Lac operator site is for illustrative purposes only, since the ideal placement of the operator may be upstream of OR1 and OR2. (b) The synthetic oscillator is coupled to the host genome by inserting the CI gene adjacent to an oscillating gene product in the host.

$$\frac{dx}{dt} = \frac{1 + x^2 + \alpha\sigma x^4}{(1 + x^2 + \sigma x^4)(1 + y^4)} - \gamma_x x\,,$$
$$\tau_y \frac{dy}{dt} = \frac{1 + x^2 + \alpha\sigma x^4}{(1 + x^2 + \sigma x^4)(1 + y^4)} - \gamma_y y\,. \quad (2)$$

The dimensionless variables are defined by $x \equiv (K_1K_4)^{1/2}X$, $y \equiv (K_2^2K_3K_6)^{1/4}Y$, and $t \equiv \sqrt{K_1K_4}\,k_t m_1 \tau$, where $m_1$ is the copy number concentration of plasmid 1. Utilizing the parameter values given in Table I, this yields $X$ (nM) $\sim 8x$, $Y$ (nM) $\sim 84y$, and $\tau$ (min) $\sim t/20$ (for a plasmid copy number concentration $m_1 = 50$ nM). The parameter $\alpha$ represents the degree to which the transcription rate is increased when a CI dimer is bound to OR2, and $\sigma$ is the affinity for a CI dimer binding to OR2 relative to binding at OR1. The time scale for the variable $y$ is set by $\tau_y \equiv (K_1^2K_4^2/K_2^2K_3K_6)^{1/4}(m_1/m_2) \sim 0.1(m_1/m_2)$, and since the copy number can be chosen for a given plasmid construct, $\tau_y$ is a design parameter. In this paper, we set $\tau_y = 5$, which is consistent with the utilization of a high-copy plasmid ($m_1 \sim 50$) for the *cI* gene and an integrated *lac* gene ($m_2 = 1$). For these copy numbers, the degradation rates are scaled such that $k_x \sim 20\gamma_x$ (min$^{-1}$) and $k_y \sim 21\gamma_y$ (min$^{-1}$). We take these parameters as tunable since degradation is a comparatively easy property to manipulate externally. In the context of our synthetic oscillator, the temperature-sensitive CI857 protein could be utilized. This protein is stable at 30 °C and becomes increasingly incapable of binding to its DNA operator sites as the temperature is increased to 42 °C. The range of the effective degradation rate from 30–42 °C is over 2 orders of magnitude [15]. Likewise, for the Lac protein, the concentration of isotropyl-$\beta$-D-thiogalactopyranoside (IPTG), which binds to Lac tetramers, can be used to induce a change in the effective Lac degradation by rendering it unable to bind to its operator site. Importantly, these manipulations are standard, and the values of $\gamma_x$ and $\gamma_y$ utilized below are easily accessible.

The plot in Fig. 2a indicates that oscillations are favored when the degradation of CI is 2–3 times that of Lac, and the bifurcation plot in Fig. 2b implies that the amplitude of the oscillations will increase with increasing $\gamma_y$. In addition, we find that the Hopf bifurcation corresponding to the upper branch in Fig. 2a is subcritical. This is highlighted in Fig. 2b, where we observe the coexistence of oscillatory and stable-state solutions for values of $\gamma_y$ about 0.037. The parameters $\alpha$ is responsible for the subcritical nature of the bifurcation (Fig. 2c), indicating that the degree of $P^*_{RM}$ activation by CI is the source of the coexistence region.

TABLE I. Synthetic network biochemical reactions. In the DNA-protein equilibrium reactions, $D^i$ denotes the promoter region of plasmid type $i$, where $i = 1, 2$. In deriving Eqs. (1) and (2), the forward equilibrium constants are defined as $K_j \equiv k_j/k_{-j}$, and the conservation law is $m_i = D^i + D^iX_2 + D^iX_2X_2 + D^iY_4 + D^iX_2Y_4 + D^iX_2X_2Y_4$, where $m_1$ ($m_2$) is the concentration of plasmid type 1 (2).

| Equilibrium reactions | Eq. constant (1/M) [Ref.] |
|---|---|
| $2X \rightleftharpoons X_2$ | $K_1 = 5 \times 10^7$ [16] |
| $4Y \rightleftharpoons 2Y_2 \rightleftharpoons Y_4$ | $K_2 = 10^8$, $K_3 = 10^7$ [25] |
| $D^i + X_2 \rightleftharpoons D^iX_2$ | $K_4 = 3 \times 10^8$ [16] |
| $D^iX_2 + X_2 \rightleftharpoons D^iX_2X_2$ | $K_5 = \sigma K_4$; $\sigma = 2$ [16] |
| $D^i + Y_4 \rightleftharpoons D^iY_4$ | $K_6 = 2 \times 10^{13}$ [26] |
| $D^iX_2 + Y_4 \rightleftharpoons D^iX_2Y_4$ | $K_7 = K_6$ |
| $D^iX_2X_2 + Y_4 \rightleftharpoons D^iX_2X_2Y_4$ | $K_8 = K_6$ |
| Production: Plasmid 1 | Rate constant |
| $D^1 \rightarrow D^1 + X$ | $k_t = 4$ min$^{-1}$ [27] |
| $D^1X_2 \rightarrow D^1X_2 + X$ | $k_t = 4$ min$^{-1}$ [27] |
| $D^1X_2X_2 \rightarrow D^1X_2X_2 + X$ | $\alpha k_t$; $\alpha = 11$ [16] |
| Production: Plasmid 2 | Rate constant |
| $D^2 \rightarrow D^2 + Y$ | $k_t = 4$ min$^{-1}$ [27] |
| $D^2X_2 \rightarrow D^2X_2 + Y$ | $k_t = 4$ min$^{-1}$ [27] |
| $D^2X_2X_2 \rightarrow D^2X_2X_2 + Y$ | $\alpha k_t$; $\alpha = 11$ [16] |

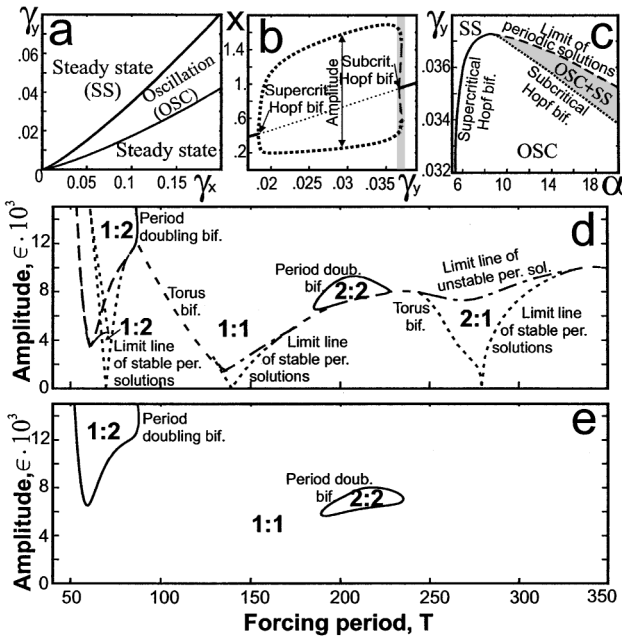


FIG. 2. Analysis of the oscillator equations (2). (a) The oscillatory region grows with increased protein degradation rates. (b) The Hopf bifurcation corresponding to the lower (upper) boundary in (a) is supercritical (subcritical). (c) The source of the subcritical bifurcation is the degree of activation. (d) The dominant Arnol'd tongue is found around the autonomous period of 147. Within this resonance region, the period of the oscillations is entrained, and is equal to the external periodic force. (e) For a system poised just outside the oscillatory region, the predominant response is 1:1 phase locking. If not plotted, parameters are fixed at $\sigma = 2$, $\alpha = 11$, $\gamma_x = 0.105$, $\gamma_y = 0.036$ (d), and $\gamma_y = 0.038$ (e).

We now turn to the employment of an intrinsic cellular process as a means of interacting with the synthetic network. We suppose there is a process in the host genome that involves oscillations in the production of protein U, and that the production of U is given by $\dot{u} = u_0 \sin\omega t$. Examples of such a process include mechanisms related to the cell division cycle or cellular motility (as in the periodic motion of flagella). In order to couple the oscillations of U to our network, the gene encoding CI is inserted adjacent to the gene encoding U (Fig. 1b). Then, since U is being transcribed periodically, the co-transcription of CI will lead to an oscillating source term in Eqs. (2), i.e., $\dot{x} = f(x, y) - \gamma_x x + \epsilon \sin(\omega t)$, where $f(x, y)$ is the nonlinear term in Eqs. (2).

We utilize the numerical bifurcation and continuation package CONT [17] to determine the boundaries of the major resonance regions. These boundaries are depicted in the parameter-space plots of Figs. 2d and 2e, where the period of the drive is plotted versus the drive amplitude for two cases: one where the synthetic network is designed with parameters just inside the oscillatory region (Fig. 2d), and one where the network lies outside the oscillatory region (Fig. 2e). In the former case, the resonance regions in Fig. 2d form the so-called Arnol'd tongues, which display an increasing range of the locking period as the amplitude of drive is increased. Outside the Arnol'd tongue regions, complex periodic and quasiperiodic solutions exist. In the latter case, we see that there is a large region of 1:1 phase locking with two small regions representing other types of simple periodic solutions.

We now consider the use of resonance in an oscillatory cellular process, and seek a strategy for amplifying its amplitude [18,19]. We focus on a network designed with parameter values just outside the oscillatory region, and study the degree to which the synthetic oscillator will respond with oscillations that are significantly greater than the drive amplitude. Viewed in this way, the synthetic network is effectively amplifying an internal cellular signal. We define the output gain by $g = A_x/\epsilon$, where $A_x$ is the amplitude of the resulting oscillations in the variable $x$. We are interested in the response of the synthetic network when its parameters are such that, without the drive, it is poised near a Hopf bifurcation. We therefore reduce the driven equations through the derivation of a normal form,

$$\dot{A} = (\tfrac{1}{2}\mu + ik_c)A + cA|A|^2 + hA|A|^4 + \epsilon \sin(\omega t) \times (c_{00} + c_{10}A + c_{01}\bar{A} + c_{20}A^2 + c_{11}|A|^2 + c_{02}\bar{A}^2 + \text{hot}), \quad (3)$$

where $A$ is a complex amplitude and the coefficients are functions of the parameters in Eqs. (2). We note that, for $\epsilon = 0$, the normal form reduces to the standard form for a Hopf bifurcation, and is to fifth order since the bifurcation is subcritical, i.e., $\mathrm{Re}(c) > 0$. Our reduction utilizes a previously reported normal form derivation [20], generalized to account for the periodic drive.

We envision designing the network so that its natural frequency is near that of the drive, with 1:1 phase locking between the drive and response. We therefore substitute $A = \mathrm{R}e^{i(\omega+\delta)t}$ into Eq. (3) and utilize the fact that $\delta \ll 1$. For a given set of parameters, the gain will depend on $\epsilon$ in a nonlinear fashion, and the normal form analysis provides a method of explicitly calculating the gain as a function of the drive amplitude. This calculation involves determining $A_x$ as a function of $\epsilon$, and the overall strategy is to first determine $A_x$ as a function of $R$, then $R$ as a function of $\epsilon$, i.e., we seek $A[R(\epsilon)]$. This is accomplished in two steps: (i) we first utilize the transformation that reduces Eqs. (2) (with drive) to the normal form Eq. (3) to obtain the amplitude of the resulting oscillations $A_x$ in terms of $R$, and (ii) we then substitute $A = \mathrm{R}e^{i(\omega+\delta)t}$ into Eq. (3), yielding $R$ in terms of $\epsilon$. In Figs. 3a and 3b, we compare the results of this calculation with the direct numerical simulation of Eqs. (2) with drive. We observe that there is an initial detuning-dependent climb in the gain, followed by a crossover to a scaling region common to all plots. In the scaling region, the theoretical calculation gives $g \sim \epsilon^{-4/5}$, and this can be directly attributed to the subcritical nature of the Hopf bifurcation.

In this Letter, we have shown how tools from nonlinear dynamics can be used to design a genetic oscillator

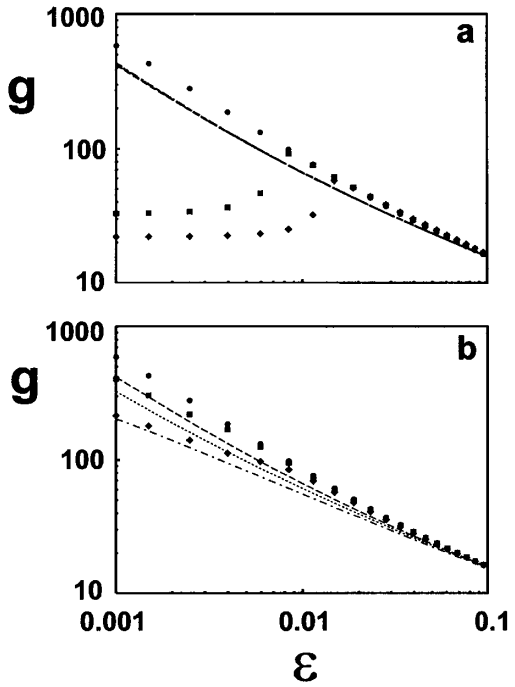


FIG. 3. Nonlinear amplification of intrinsic cellular oscillations. Results for the gain as a function of the drive amplitude generated from both the normal form analysis and direct simulation of Eqs. (2) with drive are presented for several "detuning" values, where $\Delta_\gamma \equiv (\gamma_y - \gamma_y^c)/\gamma_y^c$ and $\Delta_\omega \equiv (\omega - \omega_0)/\omega_0$ measure the amount the system is detuned from the critical point and resonance, respectively. (a) Numerical simulations for $\Delta_w = 0$ and $\Delta_\gamma = 0$ (circles), 0.1 (squares), and 0.2 (diamonds). The theoretical curves are indistinguishable for the three values of $\Delta_\gamma$. (b) Numerical simulations for $\Delta_\gamma = 0$ and $\Delta_\omega = 0.01$ (circles), 0.1 (squares), and 0.2 (diamonds). The theoretical curves correctly identify the trend away from scaling as the detuning is increased. The fixed parameters used for these plots are $\gamma_x = 0.105$, $\tau = 5$, and $\alpha = 11$.

network. We have described the coupling of the network to a periodic process that is intrinsic to the cell, and analyzed the resulting behavior in the context of synchronization. Such coupling could lead to possible strategies for entraining or inducing network oscillations in cellular protein levels, and prove useful in the design of networks which interact with cellular processes that require amplification or precise timing. Fluctuations in expression states are inherent in gene regulatory networks [8,21–24], and significant variations in oscillatory phases and amplitudes were observed in the previous synthetic oscillator study [8]. Importantly, since our proposed synthetic oscillator is designed to faithfully entrain to a cellular periodic process, such inherent fluctuations in the synthetic network will be suppressed.

We thank Farren Isaacs for discussions relating to the specific design of the CI-Lac synthetic network, and William Blake, David McMillen, and Mads Kaern for additional insightful discussions. This work was supported by the Fetzer Institute, the Office of Naval Research, the NSF, and the Dutch Science Organization.

[1] L. Glass and S. A. Kauffman, J. Theor. Biol. **39**, 103 (1973).
[2] M. A. Savageau, Nature (London) **252**, 546 (1974).
[3] P. Smolen, D. A. Baxter, and J. H. Byrne, Neuron **26**, 567 (2000).
[4] J. Hasty, D. McMillen, F. Isaacs, and J. J. Collins, Nat. Rev. Genetics **2**, 268 (2001).
[5] J. Monod, J. Wyman, and J. P. Changeux, J. Mol. Biol. **12**, 88 (1965).
[6] A. Novick and M. Weiner, Proc. Natl. Acad. Sci. U.S.A. **43**, 553 (1957).
[7] T. S. Gardner, C. R. Cantor, and J. J. Collins, Nature (London) **403**, 339 (2000).
[8] M. B. Elowitz and S. Leibler, Nature (London) **403**, 335 (2000).
[9] A. Becksei and L. Serrano, Nature (London) **405**, 590 (2000).
[10] N. Barkai and S. Leibler, Nature (London) **403**, 267 (2000).
[11] B. Novak and J. J. Tyson, Proc. Natl. Acad. Sci. U.S.A. **94**, 9147 (1997).
[12] H. H. McAdams and L. Shapiro, Science **269**, 650 (1995).
[13] D. Bray, Nature (London) **376**, 307 (1995).
[14] J. Hasty, F. Isaacs, M. Dolnik, D. McMillen, and J. J. Collins, Chaos **11**, 207 (2001).
[15] A. Villaverde, A. Benito, E. Viaplana, and R. Cubarsi, Appl. Environ. Microbiol. **59**, 3485 (1993); H. Lowman and M. Bina, Gene **96**, 133 (1990).
[16] M. Ptashne, *A Genetic Switch: Phage λ and Higher Organisms* (Cell, Cambridge, MA, 1992).
[17] M. Marek and I. Schreiber, *Chaotic Behavior of Deterministic Dissipative Systems* (Cambridge University Press, Cambridge, UK, 1991).
[18] S. Camalet, T. Duke, F. Julicher, and J. Prost, Proc. Natl. Acad. Sci. U.S.A. **97**, 3183 (2000).
[19] V. M. Eguiluz, M. Ospeck, Y. Choe, A. J. Hudspeth, and M. O. Magnasco, Phys. Rev. Lett. **84**, 5232 (2000).
[20] C. Elphick, E. Tirapegui, M. E. Brachet, P. Coullet, and G. Iooss, Physica (Amsterdam) **29D**, 95 (1987).
[21] A. Arkin, J. Ross, and H. H. McAdams, Genetics **149**, 1633 (1998).
[22] M. Thattai and A. van Oudenaarden, Proc. Natl. Acad. Sci. U.S.A. **98**, 8614 (2001).
[23] T. Kepler and T. Elston, Biophys. J. **81**, 3116 (2001).
[24] F. Isaacs, J. Hasty, C. Cantor, and J. Collins (to be published).
[25] M. Hsieh and M. Brenowitz, J. Biol. Chem. **35**, 22 092 (1997).
[26] B. Lewin, in *Genes VI* (Oxford University Press, Oxford, 1997).
[27] The bulk rate of transcription and translation is unknown. The stated value is from a consistency argument used in the context of a model describing the lysogenic state of lambda phage. See also Refs. [14,24].